Traumatic Brain Injury Causes Endothelial Dysfunction in the Systemic Microcirculation through Arginase-1-Dependent Uncoupling of Endothelial Nitric Oxide Synthase

DOI:
10.1089/neu.2015.4340

Document Version
Accepted author manuscript

Traumatic brain injury causes endothelial dysfunction in the systemic microcirculation through arginase-1–dependent uncoupling of endothelial nitric oxide synthase

[1]Nuria Villalba, PhD; [2]Adrian M. Sackheim, BSc; [2]Ivette A. Nunez, MSc; [1]David C. Hill-Eubanks, PhD; [1,2,3]Mark T. Nelson, PhD; [1,2]George C. Wellman, PhD; [1,2]Kalev Freeman, MD, PhD

[1]Department of Pharmacology, University of Vermont, Burlington, Vermont, USA

[2]Department of Surgery, University of Vermont, Burlington, Vermont, USA

[3]Institute of Cardiovascular Sciences, University of Manchester, UK

Address correspondence to:

Kalev Freeman, M.D., Ph.D.

Department of Surgery, University of Vermont, Given E301, Burlington, VT, USA, 05405.

Phone: (+1) 802 656 3410; Fax: (+1) 802 656 0680

E-mail: Kalev.Freeman@uvm.edu

Running title: Endothelial dysfunction and brain injury

Table of Contents title: Systemic endothelial dysfunction following traumatic brain injury

Key words: traumatic brain injury; in vitro studies; oxidative stress; vascular reactivity; vascular injury

Abstract

Endothelial dysfunction is a hallmark of many chronic diseases, including diabetes and long-term hypertension. Here, we show that acute traumatic brain injury (TBI) leads to endothelial dysfunction in rat mesenteric arteries. Endothelial-dependent dilation was greatly diminished 24 hours following TBI owing to impaired nitric oxide (NO) production. The activity of arginase, which competes with endothelial NO synthase (eNOS) for the common substrate L-arginine, were also significantly increased in arteries, suggesting that arginase-mediated depletion of L-arginine underlies diminished NO production. Consistent with this, substrate restoration by exogenous application of L-arginine or inhibition of arginase recovered endothelial function. Moreover, evidence for increased reactive oxygen species (ROS) production, a consequence of L-arginine starvation-dependent eNOS uncoupling, was detected in endothelium and plasma. Collectively, our findings demonstrate endothelial dysfunction in a remote vascular bed after TBI, manifesting as impaired endothelial-dependent vasodilation, with increased arginase activity, decreased generation of NO, and increased O_2^- production. We conclude that blood vessels have a "molecular memory" of neurotrauma, 24 hours after injury, due to functional changes in vascular endothelial cells; these effects are pertinent understanding the systemic inflammatory response that occurs after TBI even in the absence of polytrauma.

Introduction

Patients with severe trauma, including traumatic brain injury (TBI), have a clinical course that is often complicated by systemic inflammation and trauma-induced coagulopathy [1]. Survivors of TBI often experience profound catecholamine surges and additional systemic complications such as hypertension, pulmonary edema, and cardiomyopathy [2-9]. Notably, endothelial dysfunction secondary to systemic inflammation and shock is widely believed to contribute to systemic complications in severe trauma [9, 10], yet there have been no studies that directly measure endothelial function in systemic blood vessels after head trauma.

Endothelial dysfunction, classically described as an impairment of agonist-induced endothelial-dependent dilation, is a hallmark of cardiovascular disease [11]. Two major mechanisms of endothelial-dependent dilation of systemic resistance arteries—both initiated by increases in endothelial cell (EC) calcium (Ca^{2+})—are the nitric oxide (NO) and endothelial-dependent hyperpolarization (EDH) pathways [12-14], which are engaged by activation of endothelial NO synthase (eNOS) and small (SK_{Ca})- and intermediate (IK_{Ca})-conductance Ca^{2+}-activated potassium channels, respectively [13, 15-17]. The release of NO from the endothelium also plays a key role in modulating vascular homeostasis, promoting vasodilation in all types of blood vessels and inhibiting platelet aggregation and adhesion [18].

NO is produced through eNOS-mediated oxidation of the amino acid L-arginine to NO and L-citrulline. This reaction requires the presence of molecular oxygen (O_2) and the cofactors adenine dinucleotide phosphate (NADPH), flavin adenine dinucleotide (FAD), flavin mononucleotide (FMN), and tetrahydrobiopterin (BH_4). Increases in the intracellular concentration of Ca^{2+} ($[Ca^{2+}]_i$) in ECs upon stimulation with agonists of G protein-coupled receptors of the $G_{q/11}$ class (GqPCRs), such as acetylcholine (ACh) and bradykinin (BK), promote calmodulin-eNOS binding and thereby stimulate NO synthesis. After release from the endothelium, NO stimulates soluble guanylate cyclase (sGC) in vascular smooth muscle cells (VSMCs), resulting in an increase in the

intracellular concentration of guanosine 3′,5′-cyclic monophosphate (cGMP), which activates protein kinase G (PKG). Activated PKG, in turn, promotes vasorelaxation through phosphorylation of a number of targets in smooth muscle cells (SMCs) [19, 20].

In a variety of different contexts, particularly pathological conditions associated with vascular complications such as diabetes [21], hypertension [22], atherosclerosis [23] and obesity [24], the delicate balance of substrate and cofactors necessary for eNOS to efficiently produce NO is disrupted. In this unbalanced state, referred to as "eNOS uncoupling", eNOS donates electrons received from NADPH to O_2 instead of its normal substrate L-arginine, resulting in the production of superoxide (O_2^-). A major contributor to eNOS uncoupling is a deficiency in the cofactor BH_4, most commonly resulting from oxidation of this fragile molecule to BH_2, which competes with BH_4 for eNOS binding but is unable to function as a cofactor [25]. Notably, eNOS competes for L-arginine with arginase, which catalyzes the final step of the urea cycle to convert L-arginine into urea and L-ornithine [26]. Accordingly, increased arginase activity can also lead to eNOS uncoupling by decreasing the availability of L-arginine for eNOS [18, 27]. Regardless of the mechanism driving eNOS uncoupling, the O_2^- produced by the uncoupled reaction can react with NO to form peroxynitrite ($ONOO^-$) [28], which can further enhance eNOS uncoupling by oxidizing BH_4. Importantly, this reaction consumes NO, decreasing existing NO levels and thereby exacerbating the decrease in NO production caused by uncoupled eNOS activity. Thus, the net result of eNOS uncoupling is diminished NO levels and impaired endothelium-dependent vasodilation.

It is generally appreciated that injuries to the brain have systemic ramifications [9]. However, the impact of TBI on systemic blood vessel function has not been directly studied, and there is a knowledge gap between clinical evidence of the effects of trauma on endothelial markers and laboratory measurement of endothelial function after trauma. To address this, we utilized a well-established TBI model to assess the functional consequences of trauma on endothelium-dependent vasodilation and pressure-induced constriction (myogenic tone) in mesenteric arteries.

Extending the previously reported link between increased arginase expression or activity and various cardiovascular pathologies, we tested the hypothesis that arginase hyperfunction and subsequent eNOS uncoupling through L-arginine depletion causes the disruption in NO production that underlies TBI-induced endothelial dysfunction in the systemic

Materials and methods

Animal models. All procedures were approved by the Institutional Animal Care and Use Committee and were performed in accord with the National Research Council's *Guide for the Care and Use of Laboratory Animals*. Adult male Sprague-Dawley rats (300–325 g; Charles River, Saint Constant, Quebec, Canada) were assigned to either TBI surgery or control treatment groups. Animals in the experimental group were anesthetized and administered a fluid-percussion injury. Primary injury was induced by a direct contusion to the brain delivered to the left cerebral hemisphere by a pendulum impacting a fluid-filled chamber connected to the intact dura through a craniotomy as described previously [29, 30]. A fluid-percussion injury was induced to a target pressure of <70 psi (pound per square inch) over a 500 msec time period; the pressure was transduced and measured in each surgery. This level allows >90 % recovery, defined as ability to maintain upright posture, ambulate, and take oral hydration, and produces a highly reproducible outcome of moderate brain injury severity in those surviving animals. These experimental animals have measurable deficits in sensorimotor coordination [30], along with significant cardiovascular [30] and cerebrovascular [29] effects[29, 30]. Control animals were subjected to scalp incisions but without the percussion injury. At 24 hours after recovery from surgery, animals were euthanized and tissues were collected for experiments.

Diameter measurement in pressurized vessels. Immediately after euthanasia, a midline laparotomy was performed and the mesentery was dissected out and placed into cold (4°C) physiological saline solution (PSS) with the following composition: 118.5 mM NaCl, 4.7 mM KCl,

24 mM $NaHCO_3$, 1.18 mM KH_2PO_4, 2.5 mM $CaCl_2$, 1.2 mM $MgCl_2$ and 11 mM glucose (pH 7.4). The mesenteric vessels were then pinned out in a silicone-lined (Sylgard 184; Dow Corning, MI, USA) dissecting dish and washed with cold PSS aerated with a 20% O_2/5% CO_2 gas mixture. Fourth- and fifth-order mesenteric arteries were dissected free from the surrounding adipose and connective tissue. For each experiment, an individual mesenteric artery was cannulated in a pressure myograph (Living Systems Instrumentation, VT, USA) containing cold PSS. The proximal end of the artery was tied to the end of a borosilicate micropipette (OD 1.2 mm; tip diameter 40–60 µm) using nylon sutures. Any blood or debris remaining in the lumen was removed by flushing the artery with 1–2 mL of cold (4°C) PSS. The distal end of the artery was then tied to an opposing micropipette in the same manner. The pressure myograph was placed on the stage of an inverted microscope (AE31; Motif, Canada) and continuously superfused (7 mL/min) with oxygenated 20% O_2/5% CO_2 PSS at 37°C. Temperature was maintained using a circulating heater bath and a water-jacketed glass heat exchanger. Intraluminal pressure during the experiment was controlled by connecting the proximal end of the pressure myograph to a pressure servo system (Living Systems Instrumentation), and blood vessel diameters were measured using edge-detection software (IonOptix, MA, USA).

Assessment of myogenic tone. After cannulating, intraluminal pressure was slowly increased to 80 mm Hg and the vessel was stretched axially to remove any buckling and to mimic physiological stretch. Vessels were allowed to equilibrate and develop spontaneous pressure-induced constriction (myogenic tone). Vessels that leaked, contained branches, or failed to develop myogenic tone were discarded. For endothelial removal, arteries were cannulated on a system in which the proximal cannula and perfusion tubing were pre-filled with 1–2 mL of air using a syringe attached to the Luer-Lok inflow port. The vessel was then tied to the proximal cannula only. The pre-loaded air bolus was flushed through using a syringe filled with cold (4°C) PSS that had been equilibrated with a 20% O_2/5% CO_2 gas mixture. After denuding the endothelium, the

vessel was flushed with distilled water and PSS, and subsequently tied to the distal cannula. The effectiveness of endothelium removal was confirmed by the absence of a response to the SK_{Ca} and IK_{Ca} channel agonist NS309 (1 μM) [31]. Endothelium denudation was considered successful if NS309 caused ≤ 15% dilation of the passive diameter. Myogenic tone at 80 mm Hg was defined as the percentage decrease in the lumen diameter of arteries compared to the passive diameter, calculated as tone (%) = $[(D_{passive}-D_{active})/D_{passive}] \times 100$, where $D_{passive}$ is the (passive) lumen diameter of the artery in Ca^{2+}-free PSS containing the Ca^{2+} channel-blocking vasodilator diltiazem (100 μM), and D_{active} is the (active) lumen diameter of the artery in Ca^{2+}-containing PSS.

Assessment of endothelial-dependent vasodilation. Endothelial function was assessed by determining the response of pressurized vessels to the endothelium-dependent vasodilator ACh. Concentration–response relationships were determined in mesenteric arteries from control and TBI rats that spontaneously developed myogenic tone by measuring responses to semi-logarithmic increases in the concentrations of ACh (1 nM to 1 μM). The relative roles of EDH and NO in mesenteric arteries following TBI were tested by incubating arteries with the competitive NOS inhibitor Nω-nitro-L-arginine (L-NNA; 100 μM) for 30 minutes prior to and during agonist treatment. For some experiments, arteries were incubated with L-sepiapterin (1 μM), the arginase inhibitor Nω-hydroxy-nor-arginine (nor-NOHA; 20 μM) or the NOS and arginase substrate, L-arginine (100 μM), for 30 minutes, followed by addition of increasing concentrations of ACh (1 nM to 1μM) in the presence of L-sepiapterin, nor-NOHA or L-arginine. The percent vasodilation was defined as the agonist-induced dilation (peak or maximal response to ACh) normalized to the difference between passive and myogenic diameter, calculated as $([D_{agonist}-D_{baseline}]/[DP-D_{baseline}]) \times 100$, where $D_{baseline}$ is the lumen diameter prior to the addition of agonist at a specific concentration.

Detection of NO levels. NO levels in mesenteric arteries were measured by fluorescence microscopy as previously described using DAF-2 DA [29, 32], a non-fluorescent compound that yields

the highly fluorescent DAF-2T upon reacting with NO [33]. Arteries were surgically opened and pinned down to the surface of a custom Sylgard-coated microscope dish with the endothelial surface oriented upwards (*en face* preparation). Arteries were pre-loaded in the dark with DAF-2 DA (5 μM) in the presence of pluronic acid (0.05%) dissolved in aerated PSS. DAF-2 DA-loaded arteries were allowed to de-esterify for 15 minutes prior to imaging. NO levels were determined in vascular smooth muscle superfused with PSS under basal conditions (unstimulated) and with ACh stimulation (10 μM) at 37°C. Images were acquired at 30 frames/s using an Andor Technology Nipkow spinning-disc confocal system coupled to a Nikon Eclipse E600 FN upright microscope equipped with a 60× water-dipping objective (numerical aperture 1.0) and an electron-multiplying charge-coupled device camera, as we have previously described [29, 34]. DAF-2T fluorescence was detected using an excitation wavelength of 488 nm, and emitted fluorescence was collected using a 527–549-nm band-pass filter. Fluorescence in collected images was assessed offline by measuring the average fluorescence of 10 images from the same field using custom-designed software (A. Bonev, University of Vermont, Burlington, VT) [34]. The area of each VSMC surface was determined by drawing a freehand region of interest (ROI) around the outline of the individual cell. Total DAF-2T fluorescence was measured over the entire area of each cell, and an average value per cell was calculated for a given field (>10 cells). DAF-2T fluorescence was expressed as the percentage change from control baseline levels.

Immunohistochemistry. Mesenteric arteries were fixed in 4% paraformaldehyde for 1 hour and then cryoprotected overnight in 0.1 M PBS (pH 7.2) containing 3% sucrose. Cross-sections of arteries were embedded in optimal cutting temperature (O.C.T.) compound, cut into 10-μm-thick slices, and mounted on poly-L-lysine–coated glass slides (Sigma-Aldrich, MO, USA). Sections were pre-incubated with PBS containing 1.6% hydrogen peroxide for 5 minutes and then washed with PBS containing 0.2% Tween-20. Endogenous biotin or avidin binding sites were blocked by sequential incubation for 10 minutes with avidin and biotin peroxidase complex (ABC kit; Vector

Laboratories, CA, USA). After rinsing, arteries were permeabilized with 0.1% Triton X-100 in PBS for 20 minutes, washed with PBS, and incubated overnight at 4°C with primary antibodies against arginase-1 (Genetex, CA, USA) or arginase-2 (Santa Cruz Biotech, TX, USA) diluted 1:200 and 1:100, respectively, in 3% bovine serum albumin (BSA). After washing again with PBS, slide-mounted artery sections were incubated with a biotin-labeled secondary antibody for 30 minutes. Immunoreactive proteins were detected by incubating with the peroxidase substrate 3,3-diaminobenzine. Negative controls were incubated with secondary antibody only (primary antibody replaced with PBS). Images were acquired at 100x magnification.

Arginase activity assay. Arginase enzymatic activity was measured in mesenteric artery homogenates obtained from control and TBI rats using a colorimetric assay kit (Sigma-Aldrich). Arginase activity was quantified by spectrophotometric measurement of urea produced by arginase from L-arginine.

Detection of O_2^- production in mesenteric arteries. Dihydroethidium (DHE) was used to identify O_2^- production *in situ* [32]. Mesenteric arteries from control and TBI rats were isolated as described above, and incubated with DHE (2 µM) in the dark in a custom humidifying box at 37°C for 30 minutes, rinsed three times with PSS for 10 minutes each, and then fixed in paraformaldehyde (4%) for 1 hour. Arteries were cryoprotected overnight in 3% sucrose and then embedded in O.C.T. mounting media. Mesenteric arteries were cut into cross-sections (10 µm thick) using a cryostat, and then immunostained for eNOS (1:2,000; BD Biosciences, CA, USA) used as an endothelial marker. A 4′-6-diamidino-2-phenylindole (DAPI) staining (1:500; Thermo Scientific) was performed for nuclear acid (nuclei) staining (excitation/emission: 350/470 nm). Images were acquired at 60x magnification using a confocal microscope (Zeiss LSM510 META) to visualize the fluorescence (excitation/emission: 518/605 nm for DHE-labeled slices). Fluorescence intensity was quantified by ImageJ software.

Oxidation-reduction production (ORP) measurements. Redox balance (integrated measure of the balance between total oxidants and reductants) was evaluated in plasma samples obtained from control and TBI rats by measuring the oxidation-reduction potential, or total oxidizing capacity [35]. Whole blood was collected at the time of euthanasia into an evacuated tube containing sodium citrate. Whole blood was immediately centrifuged (2,000 r.p.m; 4 °C), and plasma samples were collected, aliquoted, and stored at -80°C. Thawed samples (30 µL) were tested using the RedoxSYS diagnostic platform, consisting of a micro Pt/AgCl combination redox electrode sensor and benchtop analyzer (Aytu Bioscience, Inc., CO, USA) [36, 37]. Values were recorded in millivolts (mV) after ORP readings were stable for 10 seconds. The diagnostic platform was calibrated before use and validated with hydrogen peroxide (30 µM) as a positive control.

Statistics. GraphPad Prism software (version 6.03; GraphPad Software, CA, USA) was used for analysis; values are presented as means ± SEM. Agonist concentration-response curves were calculated by fitting the Hill slope from the data (variable slope model) for each individual experiment, and summary data are presented for inter-group comparisons together with representative tracings. The Mann-Whitney nonparametric test was used for comparisons between two experimental groups. Two-way analysis of variance (ANOVA) was used for comparisons of multiple group measurements at different concentrations. The α-value used was 0.05, and statistical significance was reported as *P*-values. In a few experimental series, a single control group was used to test multiple hypotheses. To avoid increasing the likelihood of a Type I error, we used the Bonferroni correction to test each individual hypothesis at a significance level determined by $\alpha = 1/m$, where m is the number of comparisons.

Results

TBI animals develop endothelial dysfunction, characterized by impaired endothelial-dependent vasodilation. In this study, we performed TBI surgery in a total of 38 animals. The average fluid-percussion injury pressure delivered to the TBI group was 68 ± 1 psi. Endothelial function was

assessed in pressurized mesenteric arteries from control and TBI rats by measuring dilatory responses to the muscarinic receptor agonist ACh. Arteries from control animals achieved maximal dilation at 300 nM ACh (Figure 1). In contrast, an ACh concentration of 1 μM was required to dilate arteries from TBI rats, and even at that concentration, the dilation achieved was only ~50% of that in controls (Figure 1; Table 1). Application of higher concentrations of ACh to arteries from TBI rats did not cause further dilation, and instead produced diminished vasodilatory responses (21% ± 11% and 10% ± 11% at 3 and 10 μM ACh, respectively, n = 4). The ACh concentration-response curve (Figure 1) demonstrates that the percent vasodilation produced by 1 μM ACh was significantly decreased in mesenteric arteries from TBI rats, whereas the calculated 50% effective concentration (EC_{50}) was unchanged (Table 1). Thus, TBI significantly impairs endothelial-dependent vasodilatory function in systemic vessels remote from the site of injury.

Impaired vasodilation after trauma is due to crippling of the NO component of endothelial-dependent vasodilation. We next sought to determine the specific pathway of endothelial-dependent vasodilation that accounted for the dysfunction observed in systemic arteries after TBI. ACh induces dilation of rat mesenteric arteries through a combination of NO and EDH mechanisms; thus, disruption of either or both pathways could be responsible for the impaired response to ACh. To identify the affected pathway(s), we blocked NO production using the NOS inhibitor L-NNA (100 μM) and examined the remaining EDH component of vasodilation. As expected, L-NNA decreased ACh-induced dilation in control arteries; however, it had no effect on the already impaired arteries from TBI animals (Table 1). Collectively, these findings suggest that impairment of the NO pathway of endothelial-mediated dilation fully accounts for the abnormal agonist-induced dilation of mesenteric arteries after TBI.

Basal and ACh-induced NO production is decreased following TBI. To determine the effects of TBI on vascular NO production, we directly measured NO under physiological conditions as the

conversion of the NO indicator DAF-2 DA to the highly fluorescent DAF-2T. Both baseline and ACh-induced NO levels in the VSMC layer, which receives NO by diffusion from the adjacent endothelium, were also significantly decreased in arteries from TBI rats compared to controls (Figure 2).

Diminished endogenous NO production following TBI impairs myogenic tone. The effect of TBI on endogenous NO in intact pressurized arteries was functionally assessed by measuring differences in vasoconstrictor responses to inhibition of NOS with L-NNA (100 μM) between TBI and control groups (Figure 3). L-NNA–induced constriction was significantly diminished in arteries from TBI rats (5% ± 1% constriction, n = 6) compared to controls (9% ± 1% constriction, n = 10; $P < 0.05$), confirming that endogenous NO synthesis is compromised following TBI (Figure 3A–C). To test whether changes in NO production observed following TBI alter arterial myogenic tone, we investigated constriction in response to pressure (80 mm Hg). Myogenic tone was significantly enhanced in endothelium-intact arteries from TBI rats (41% ± 7%, n = 8) compared with controls (25% ± 3%, n = 9; $P < 0.05$; Figure 3D). Both endothelium removal and treatment with L-NNA significantly increased constriction in response to pressure in control mesenteric arteries (Figure 3D), consistent with the idea that NO is endogenously produced in the vascular endothelium of mesenteric arteries and modulates the myogenic response under normal physiological conditions. In contrast, neither endothelium denudation nor L-NNA treatment significantly affected myogenic tone in arteries from TBI rats (Figure 3D), implying a virtual absence of tonic NO release by mesenteric artery ECs from TBI rats. Notably, both removal of the endothelium and inhibition of eNOS with L-NNA normalized the level of myogenic tone between control and TBI mesenteric arteries (Figure 3D). Lumen diameters at 80 mm Hg under Ca^{2+}-free conditions were not significantly different between intact arteries from control (238 ± 10 μm, n = 9) and TBI (220 ± 18 μm, n = 8) rats. Moreover, neither the sensitivity of vascular smooth muscle to NO, tested using the NO donor spermine NONOate (0.001–1 μM) in the presence of

L-NNA (100 μM), nor contractility to the TXA_2 agonist U46619 (0.001–0.3 μM) were significantly different between groups (Figure 4). Collectively, these data indicate that diminished endothelial release of NO fully accounts for the impaired myogenic response in arteries from TBI rats.

Arginase inhibition and exogenous supplementation of BH_4 or L-arginine improves agonist-induced dilation following TBI. Inadequate or uncoupled eNOS function leads to O_2^- production, a hallmark of endothelial dysfunction in vascular disease [18]. We therefore hypothesized that the diminished NO component of vasodilation after trauma is due to eNOS uncoupling, through depletion of the eNOS co-factor BH_4 and/or its substrate L-arginine. First, to test the contribution of BH_4 depletion to eNOS uncoupling, we treated arteries with the pterin salvage pathway-derived precursor L-sepiapterin (1 μM). L-sepiapterin partially restored vasodilation induced by ACh; although the EC_{50} was not affected, the maximal dilation induced by 1 μM ACh in the presence of L-sepiapterin was improved, and reached approximately 90% of control levels (Figure 5 and Table 1). Next, we found that supplementation with L-arginine (100 μM) and arginase inhibition with nor-NOHA (20 μM) vastly improved the impaired endothelial-dependent dilation in mesenteric arteries from TBI rats (Figure 6 and Table 1). This suggested the possibility that activation of arginase after TBI, and subsequent starvation of eNOS of the common substrate L-arginine, is responsible for diminished NO and vasodilatory capacity. It should be noted that, in mesenteric arteries from control rats, administration of nor-NOHA, L-arginine, or L-sepiapterin diminished NO-mediated dilation to ACh instead of enhancing it, a phenomenon termed the "arginase paradox" that has been observed previously (see Discussion).

TBI increases arginase activity in mesenteric arteries. Since arginase inhibition improved endothelial-dependent vasodilation after trauma, we evaluated arginase activity in mesenteric arteries from control and TBI rats. Arginase enzymatic activity was strikingly elevated in homogenates of TBI mesenteric arteries (1 ± 0.5 units/L, n = 5) compared with controls (0.1 ± 0.05 units/L, n = 4; $P < 0.05$) (Figure 7A). By contrast, arginase activity in liver was not significantly

different between control (8 ± 0.1 units/L, n = 5) and TBI (7 ± 0.3 units/L, n = 4) groups. Furthermore, we found the isoform arginase-1 expressed in the vascular endothelium (Figure 7B).

Increased superoxide production provides further evidence for eNOS uncoupling after TBI. Finally, we examined whether arginase-mediated eNOS uncoupling contributes to enhanced reactive oxygen species (ROS) production following TBI. We detected O_2^- production in the vascular endothelium and increased oxidative stress in circulating plasma in both groups. Using confocal microscopy in conjunction with the O_2^- indicator DHE, we found an overall increase in intracellular O_2^- production in the vascular endothelium of mesenteric arteries from TBI rats (Figure 8A–B). Moreover, oxidation-reduction potential (ORP), a measure of total oxidative stress [36, 37], was higher in plasma collected from TBI rats (183 ± 13 mV, n = 6) than control rats (154 ± 3 mV, n = 5) (Figure 8C, D).

Discussion

Here we demonstrated that TBI causes endothelial dysfunction in the systemic microcirculation, and provide novel insight into the underlying mechanisms. Our findings strongly support a model in which TBI increases arginase activity, which competes with eNOS for L-arginine and thus limits L-arginine bioavailability for NO production. This decreased substrate availability leads to eNOS uncoupling, resulting in O_2^- generation and endothelial dysfunction (Figure 9).

We found that after TBI, endothelial-dependent responses to ACh (Figure 1) were severely impaired in myogenically active, small mesenteric arteries. L-NNA, an inhibitor of endogenous NO production, blunted dilation to ACh (by ~50%) in pressurized arteries from control rats but had no effect in arteries from TBI rats, indicating that this diminished response is due to a loss of the NO component of endothelium-dependent vasodilation (Figure 3). Consistent with this, basal endogenous NO production in endothelium-intact vessels from TBI animals was significantly reduced, resulting in enhanced myogenic tone (Figures 2 and 3). Collectively, these findings implicate impaired NO production after TBI in the observed vascular dysfunction. This conclusion

is further supported by our observation that differences in myogenic tone between TBI and control arteries were eliminated by endothelial denudation and L-NNA treatment.

Despite the fact that L-arginine concentrations within the cell are already saturating (100–1000 μM), eNOS-mediated NO synthesis can be boosted by increasing the extracellular L-arginine concentration [38-40], a phenomenon known as the "arginine paradox". In this context, we found that endothelial-dependent dilation of mesenteric arteries from TBI rats was improved by suppressing L-arginine degradation through inhibition of arginase with nor-NOHA or by exogenous addition of L-arginine (Figure 6). In contrast, L-arginine supplementation and arginase inhibition diminished the response to ACh in mesenteric arteries from control rats. These observations support the paradoxical effect of manipulations that increase L-arginine levels: though beneficial in the context of vascular dysfunction, they exert a detrimental effect on NO production and endothelial function in healthy controls [41]. As a practical matter, the manifestations of this paradox also create challenges for evaluating and interpreting the results of pharmacological interventions in control and TBI groups. In a conventional experimental design, inferring specific treatment effects in experimental groups is predicated on the idea that treatments have minimal, or at least qualitatively similar, effects on controls. The fact that L-sepiapterin, L-arginine and nor-NOHA diminished responses to ACh in controls such that these responses actually overlapped with the enhanced response to treatment in the experimental (TBI) group upends this presumption. Our decision to present results in control and TBI groups with and without treatment rather than compare control-treated and TBI-treated groups reflects this experimental conundrum, which is inherent in manipulations of the eNOS–arginase system.

A corollary of the arginine paradox is that decreases in intracellular levels of L-arginine can attenuate eNOS activity; it has also been shown that L-arginine depletion can result in eNOS uncoupling in the vascular endothelium [42]. This depletion of substrate can be attributed to an increase in the activity of arginase, which siphons off L-arginine and starves eNOS of its substrate, resulting in reduced production of NO and increased production of O_2^-. Consistent with this

mechanism, we found that arginase activity was increased in mesenteric artery homogenates from TBI rats. Downstream elements within the NO signaling pathway were also unaffected, as evidenced by the fact that endothelial-independent vasodilation in response to the NO donor spermine NONOate was unchanged between groups. Contractility in response to the thromboxane agonist U46619 was also preserved after TBI. These observations rule out altered NO sensitivity or smooth muscle dysfunction as mechanisms of impaired vasodilation. Thus, our findings support the idea that eNOS is the "loser" in the competition between eNOS and arginase for L-arginine, with the result being diminished NO production, eNOS uncoupling, and increased formation of O_2^- and $ONOO^-$, the latter of which is predicted to further decrease NO levels (by consuming existing NO) and potentiate eNOS uncoupling (by oxidizing BH_4). Interestingly, supplementation with L-sepiapterin, an intermediate in the salvage pathway of BH_4 synthesis, partially improved ACh-induced vasodilation at the maximal concentration used (1 μM), suggesting that a decrease in BH_4 concentration, possibly reflecting $ONOO^-$-mediated oxidation to BH_2, may also contribute to diminished eNOS activity [22].

The arginine paradox described above can be explained in part by differences in the enzyme kinetics of arginase and eNOS [41, 43]. The K_m of eNOS for L-arginine in intact cells (2–20 μM) is 1000-fold lower than that of arginase (2–20 mM) [39]; however, the maximum activity (V_{max}) of arginase is 1000-fold higher than that of eNOS, allowing the two enzymes to compete equally for the same substrate if they are located in the same cellular microdomain [44, 45]. In addition, the K_m of eNOS for L-arginine is comparable to that of the cationic amino acid transporter 1 (CAT1) responsible for L-arginine transport (100–150 μM) [46], suggesting that NO production through eNOS is not only reciprocally regulated by arginase, but also by L-arginine transport into the cell. Taken together, the enzymatic properties of eNOS, arginase, L-arginine transport mechanisms, and concentration gradients comprise an elegant, very tightly controlled system for regulating the metabolism of L-arginine. Our findings are in accord with previous reports that arginase activity is increased and extracellular L-arginine is decreased in both animal models and human subjects

after trauma [47, 48]. These studies have also shown a correlation between arginase activity and the severity of an injury [47, 48], with modest increases (1.5- to 2-fold) being reported after minor elective surgery and much greater increases (~10-fold) occurring after severe trauma [47, 48]. Although these observations would seem to suggest L-arginine supplementation as a therapeutic strategy, several studies have shown that L-arginine reactivity varies depending on time point after injury, vascular bed and species studied, age and the underlying disease [48-53]. One of the limitations of our study is that we focused on a specific time point after injury. Additional studies are needed to address the longitudinal course of vascular responses including earlier times after TBI, and later time points following clinical recovery.

Using the O_2^- indicator DHE, we found that TBI caused excessive O_2^- production in endothelial cells. We further found that TBI induced sufficient systemic inflammation and oxidative stress at 24 hours to produce a detectable ORP signal in the circulating plasma. Similar ORP increases were recently reported in humans with severe trauma, specifically TBI [36, 37]. Our results suggest that L-arginine depletion and eNOS uncoupling associated with TBI are responsible for the increase in endothelial ROS, which would place ROS elevation downstream of arginase and L-arginine depletion. Our working hypothesis is that pro-inflammatory cytokines, such as TNF-α, IL-4, IL-10 and IL-13, which are elevated in the circulation following TBI and have been implicated in increasing arginase activity or expression [47, 54], are responsible for the observed endothelial dysfunction. In a similar manner, increases in endothelial O_2^- (e.g., derived from NADPH oxidase [22, 55], xanthine oxidase [56, 57] or mitochondrial respiration [58] could act early in the process to initiate eNOS uncoupling through oxidation of BH_4, making increased arginase activity and subsequent L-arginine depletion a contributing rather than initiating event. Moreover, our data do not allow us to determine whether endothelial O_2^- is a major contributor to the increased ORP signal in plasma or whether other cellular sources are primarily responsible. In this context, there is

substantial evidence for the release of ROS in addition to pro-inflammatory cytokines by activated platelets and macrophages after trauma [1].

NO plays a major role in the pathophysiology of TBI. Changes in NOS isoenzyme expression and tissue NO levels appear to be time dependent and complex [59]. We recently investigated the effects of TBI in cerebral arteries, and found that the responses were opposite those in systemic arteries [29]. Instead of a decrease in NO, cerebral arteries from the same trauma model showed a 60-fold increase in NO at the same time point, leading to a gain of NO function and a loss of myogenic tone [29]. The dramatically different responses of cerebral and mesenteric artery endothelium reflect fundamental differences in the cellular consequences of TBI. We suspect that the specialized cerebrovascular endothelium, which constitutes the blood-brain barrier, may also protect these vessels from toxic or inflammatory effects of circulating factors such as cytokines [60] and damage-associated molecular patterns (DAMPs) or alarmins such as extracellular histones from apoptotic cells [61, 62] released into the blood stream by TBI-induced cellular damage. There are several possible mechanisms by which the cerebrovascular endothelium could protect against inflammation and eNOS uncoupling, including differences in cell surface receptors, intracellular modulators of NO signaling, superoxide dismutase activity, and astroglial interactions. In this context, the inflammation initiated in the injured brain proliferates throughout the body, turning an isolated event into a systemic pathology.

In conclusion, we show increased arginase activity and eNOS uncoupling through L-arginine depletion causes a disruption in NO production that underlies TBI-induced endothelial dysfunction in the systemic microcirculation. We provides a mechanism by which small blood vessels “remember” an injury 24 hours after the acute event, even after removal from the body, supporting a model of “molecular memory” in vascular endothelial cells after neurotrauma. These results are relevant to understanding the systemic inflammatory response that occurs after TBI even in the absence of polytrauma. Although we cannot exclude other, and perhaps overlapping, mechanisms of endothelial dysfunction, it is clear that TBI causes profound effects on the

systemic microcirculation and these responses are opposite to those in cerebral arteries. By elucidating the underlying mechanisms that cause acute endothelial dysfunction following a head injury, our findings may inform strategies for endothelial protection and prevention of coagulopathy in the management of brain trauma.

Acknowledgments

We thank Sheila Russell for her technical expertise in performing the trauma surgeries. This work was supported by the Totman Medical Research Trust, Fondation Leducq and National Institutes of Health (P20-RR-16435, P01-HL-095488, UM1-HL-120877-01, R01-HL-044455, R01-HL-098243, R37-DK-053832, P30-RR-032135-02, P30-GM-103498-02, K08-GM-098795-01, R01-HL-121706-01).

Author Disclosure Statement

None

References

1. Mann KG, F.K. (2015). TACTIC: Trans-agency consortium for trauma-induced coagulopathy. J. Thromb. Haemost.

2. Hortnagl, H., Hammerle, A.F., Hackl, J.M., Brucke, T., Rumpl, E. and Hortnagl, H. (1980). The activity of the sympathetic nervous system following severe head injury. Intensive Care Med. 6, 169--167.

3. Clifton, G.L., Ziegler, M.G. and Grossman, R.G. (1981). Circulating catecholamines and sympathetic activity after head injury. Neurosurgery 8, 10-14.

4. Clifton, G.L., Robertson, C.S., Kyper, K., Taylor, A.A., Dhekne, R.D. and Grossman, R.G. (1983). Cardiovascular response to severe head injury. J. Neurosurg. 59, 447-454.

5. Woolf, P.D., Hamill, R.W., Lee, L.A., Cox, C. and McDonald, J.V. (1987). The predictive value of catecholamines in assessing outcome in traumatic brain injury. J. Neurosurg. 66, 875-882.

6. Rosner, M.J., Newsome, H.H. and Becker, D.P. (1984). Mechanical brain injury: the sympathoadrenal response. J. Neurosurg. 61, 76-86.

7. Gaetz, M. (2004). The neurophysiology of brain injury. Clin. Neurophysiol. 115, 4-18.

8. Bybee, K.A. and Prasad, A. (2008). Stress-related cardiomyopathy syndromes. Circulation 118, 397-409.

9. Gaddam, S.S., Buell, T. and Robertson, C.S. (2015). Systemic manifestations of traumatic brain injury. Handb. Clin. Neurol. 127, 205-218.

10. Maegele, M., Schochl, H. and Cohen, M.J. (2014). An update on the coagulopathy of trauma. Shock 41 Suppl 1, 21-25.

11. Endemann, D.H. and Schiffrin, E.L. (2004). Endothelial dysfunction. J. Am. Soc. Nephrol. 15, 1983-1992.

12. Palmer, R.M., Ferrige, A.G. and Moncada, S. (1987). Nitric oxide release accounts for the biological activity of endothelium-derived relaxing factor. Nature 327, 524-526.

13. Bryan, R.M., You, J., Golding, E.M. and Marrelli, S.P. (2005). Endothelium-derived hyperpolarizing factor: a cousin to nitric oxide and prostacyclin. Anesthesiology 102, 1261-1277.

14. Edwards, G., Félétou, M. and Weston, A.H. (2010). Endothelium-derived hyperpolarising factors and associated pathways: a synopsis. Pflugers Arch. 459, 863-879.

15. Brayden, J. and Nelson, M. (1992). Regulation of arterial tone by activation of calcium-dependent potassium channels. Science 256, 532.

16. Crane, G.J., Gallagher, N., Dora, K.A. and Garland, C.J. (2003). Small- and intermediate-conductance calcium-activated K+ channels provide different facets of endothelium-dependent hyperpolarization in rat mesenteric artery. The Journal of Physiology 553, 183-189.

17. Taylor, M.S., Bonev, A.D., Gross, T.P., Eckman, D.M., Brayden, J.E., Bond, C.T., Adelman, J.P. and Nelson, M.T. (2003). Altered expression of small-conductance Ca2+-activated K+ (SK3) channels modulates arterial tone and blood pressure. Circ. Res. 93, 124-131.

18. Forstermann, U. and Sessa, W.C. (2012). Nitric oxide synthases: regulation and function. Eur. Heart J. 33, 829-837, 837a-837d.

19. Walsh, M.P., Kargacin, G.J., Kendrick-Jones, J. and Lincoln, T.M. (1995). Intracellular mechanisms involved in the regulation of vascular smooth muscle tone. Can. J. Physiol. Pharmacol. 73, 565-573.

20. Moncada, S., Palmer, R.M. and Higgs, E.A. (1991). Nitric oxide: physiology, pathophysiology, and pharmacology. Pharmacol. Rev. 43, 109-142.

21. Settergren M, Bohm, F., Malmstrom, R.E., Channon, K.M. and Pernow, J. (2009). L-arginine and tetrahydrobiopterin protects against ischemia/reperusion induce endothelial dysfunction in patients with type 2 diabetes mellitus and coronary artery disease. Atherosclerosis 204, 73-78.

22. Landmesser, U., Dikalov, S., Price, S., McCann, L., Fukai, T., Holland, S., Mitch, W. and Harrison, D. (2003). Oxidation of tetrahydrobiopterin leads to uncoupling of endothelial cell nitric oxide synthase in hypertension. The Journal of clinical investigation 111, 1201-1209.

23. Shemyakin, A., Kovamess, O., Rafnsson, A., Bohm, F., Svenarud, P., Stettergren, M., Jun, C. and Pernow, J. (2012). Arginase inhibition improves endotheliul function in patients with coronary artery disease and type 2 diabetes melliuts. Circulation 126, 2943-2950.

24. Yu, Y., Rajapakse, A.G., Montani, J., Yang, Z. and Ming, X. (2014). p38 mitogen-activated protein kinase is involved in arginase-II-mediated eNOS-Uncoupling in Obesity. Cardiovasc Diabetology 13, 113.

25. Alkaitis, M.S. and Crabtree, M.J. (2012). Recoupling the cardiac nitric oxide synthases: tetrahydrobiopterin synthesis and recycling. Curr. Heart Fail. Rep. 9, 200-210.

26. Jenkinson, C.P., Grody, W.W. and Cederbaum, S.D. (1996). Comparative properties of arginases. Comp. Biochem. Physiol. B Biochem. Mol. Biol. 114, 107-132.

27. Feletou, M. and Vanhoutte, P.M. (2007). Endothelium-dependent hyperpolarizations: past beliefs and present facts. Ann. Med. 39, 495-516.

28. Rochette, L., Lorin, J., Zeller, M., Guilland, J., Lorgis, L., Cottin, Y. and Vergely, C. (2013). Nitric oxide synthase inhibition and oxidative stress in cardiovascular diseases: Possible therapeutic target? Pharmacol Ther 140.

29. Villalba, N., Sonkusare, S.K., Longden, T.A., Tran, T.L., Sackheim, A.M., Nelson, M.T., Wellman, G.C. and Freeman, K. (2014). Traumatic brain injury disrupts cerebrovascular tone through endothelial inducible nitric oxide synthase expression and nitric oxide gain of function. Journal of the American Heart Association 3, e001474.

30. Larson, B.E., Stockwell, D.W., Boas, S., Andrews, T., Wellman, G.C., Lockette, W. and Freeman, K. (2012). Cardiac reactive oxygen species after traumatic brain injury. J. Surg. Res. 173, e73-81.

31. Hannah, R.M., Dunn, K.M., Bonev, A.D. and Nelson, M.T. (2011). Endothelial SK(Ca) and IK(Ca) channels regulate brain parenchymal arteriolar diameter and cortical cerebral blood flow. J Cereb Blood Flow Metab 31, 1175-1186.

32. Arribas, S.M., Gonzalez, J.M., Briones, A.M., Somoza, B., Daly, C.J., Vila, E., Gonzalez, M.C. and McGrath, J.C. (2007). Confocal myography for the study of hypertensive vascular remodelling. Clin. Hemorheol. Microcirc. 37, 205-210.

33. Kojima, H., Sakurai, K., Kikuchi, K., Kawahara, S., Kirino, Y., Nagoshi, H., Hirata, Y. and Nagano, T. (1998). Development of a fluorescent indicator for nitric oxide based on the fluorescein chromophore. Chem Pharm Bull 46, 373-375.

34. Sonkusare, S.K., Bonev, A.D., Ledoux, J., Liedtke, W., Kotlikoff, M.I., Heppner, T.J., Hill-Eubanks, D.C. and Nelson, M.T. (2012). Elementary Ca2+ signals through endothelial TRPV4 channels regulate vascular function. Science 336, 597-601.

35. Shapiro, H.M. (1972). Redox balance in the body: an approach to quantitation. J. Surg. Res. 13, 138-152.

36. Rael, L.T., Bar-Or, R., Mains, C.W., Slone, D.S., Levy, A.S. and Bar-Or, D. (2009). Plasma oxidation-reduction potential and protein oxidation in traumatic brain injury. J. Neurotrauma 26, 1203-1211.

37. Rael, L.T., Bar-Or, R., Salottolo, K., Mains, C.W., Slone, D.S., Offner, P.J. and Bar-Or, D. (2009). Injury severity and serum amyloid A correlate with plasma oxidation-reduction potential in multi-trauma patients: a retrospective analysis. Scandinavian journal of trauma, resuscitation and emergency medicine 17, 57.

38. Li, H., Meininger, C.J., Hawker, J.R., Jr., Haynes, T.E., Kepka-Lenhart, D., Mistry, S.K., Morris, S.M., Jr. and Wu, G. (2001). Regulatory role of arginase I and II in nitric oxide, polyamine, and proline syntheses in endothelial cells. Am. J. Physiol. Endocrinol. Metab. 280, E75-82.

39. Wu, G. and Morris, S.M., Jr. (1998). Arginine metabolism: nitric oxide and beyond. Biochem. J. 336 (Pt 1), 1-17.

40. Dhanakoti, S.N., Brosnan, J.T., Herzberg, G.R. and Brosnan, M.E. (1990). Renal arginine synthesis: studies in vitro and in vivo. Am. J. Physiol. 259, E437-442.

41. Dioguardi, F.S. (2011). To give or not to give? Lessons from the arginine paradox. Journal of nutrigenetics and nutrigenomics 4, 90-98.

42. Landmesser, U., Dikalov, S., Price, S.R., McCann, L., Fukai, T., Holland, S.M., Mitch, W.E. and Harrison, D.G. (2003). Oxidation of tetrahydrobiopterin leads to uncoupling of endothelial cell nitric oxide synthase in hypertension. J. Clin. Invest. 111, 1201-1209.

43. Bode-Boger, S.M., Scalera, F. and Ignarro, L.J. (2007). The L-arginine paradox: Importance of the L-arginine/asymmetrical dimethylarginine ratio. Pharmacol. Ther. 114, 295-306.

44. Reczkowski, R.S. and Ash, D.E. (1994). Rat liver arginase: kinetic mechanism, alternate substrates, and inhibitors. Arch. Biochem. Biophys. 312, 31-37.

45. Griffith, O.W. and Stuehr, D.J. (1995). Nitric oxide synthases: properties and catalytic mechanism. Annu. Rev. Physiol. 57, 707-736.

46. Granger, D.L., Hibbs, J.B., Jr., Perfect, J.R. and Durack, D.T. (1990). Metabolic fate of L-arginine in relation to microbiostatic capability of murine macrophages. J. Clin. Invest. 85, 264-273.

47. Ochoa, J.B., Bernard, A.C., O'Brien, W.E., Griffen, M.M., Maley, M.E., Rockich, A.K., Tsuei, B.J., Boulanger, B.R., Kearney, P.A. and Morris Jr, S.M., Jr. (2001). Arginase I expression and activity in human mononuclear cells after injury. Ann. Surg. 233, 393-399.

48. Pribis, J.P., Zhu, X., Vodovotz, Y. and Ochoa, J.B. (2012). Systemic arginine depletion after a murine model of surgery or trauma. JPEN J. Parenter. Enteral Nutr. 36, 53-59.

49. Schulman, S.P., Becker, L.C., Kass, D.A., Champion, H.C., Terrin, M.L., Forman, S., Ernst, K.V., Kelemen, M.D., Townsend, S.N., Capriotti, A., Hare, J.M. and Gerstenblith, G. (2006). L-arginine therapy in acute myocardial infarction: the Vascular Interaction With Age in Myocardial Infarction (VINTAGE MI) randomized clinical trial. JAMA 295, 58-64.

50. Rangel-Castilla, L., Ahmed, O., Goodman, J.C., Gopinath, S., Valadka, A. and Robertson, C. (2010). L-arginine reactivity in cerebral vessels after severe traumatic brain injury. Neurol. Res. 32, 1033-1040.

51. Zimmermann, C., Wimmer, M. and Haberl, R.L. (2004). L-arginine-mediated vasoreactivity in patients with a risk of stroke. Cerebrovasc. Dis. 17, 128-133.

52. Okamoto, M., Etani, H., Yagita, Y., Kinoshita, N. and Nukada, T. (2001). Diminished reserve for cerebral vasomotor response to L-arginine in the elderly: evaluation by transcranial Doppler sonography. Gerontology 47, 131-135.

53. Liu, H., Goodman, J.C. and Robertson, C.S. (2002). The effects of L-arginine on cerebral hemodynamics after controlled cortical impact injury in the mouse. J. Neurotrauma 19, 327-334.

54. Liu, Y., Gardner, C.R., Laskin, J.D. and Laskin, D.L. (2013). Classical and alternative activation of rat hepatic sinusoidal endothelial cells by inflammatory stimuli. Exp. Mol. Pathol. 94, 160-167.

55. Rajagopalan, S., Kurz, S., Munzel, T., Tarpey, M., Freeman, B.A., Griendling, K.K. and Harrison, D.G. (1996). Angiotensin II-mediated hypertension in the rat increases vascular superoxide production via membrane NADH/NADPH oxidase activation. Contribution to alterations of vasomotor tone. J. Clin. Invest. 97, 1916-1923.

56. Ohara, Y., Peterson, T.E. and Harrison, D.G. (1993). Hypercholesterolemia increases endothelial superoxide anion production. J. Clin. Invest. 91, 2546-2551.

57. Alef, M.J., Vallabhaneni, R., Carchman, E., Morris, S.M., Jr., Shiva, S., Wang, Y., Kelley, E.E., Tarpey, M.M., Gladwin, M.T., Tzeng, E. and Zuckerbraun, B.S. (2011). Nitrite-generated NO circumvents dysregulated arginine/NOS signaling to protect against intimal hyperplasia in Sprague-Dawley rats. J. Clin. Invest. 121, 1646-1656.

58. Murphy, M.P. (2009). How mitochondria produce reactive oxygen species. Biochem. J. 417, 1-13.

59. Cherian, L., Hlatky, R. and Robertson, C.S. (2004). Nitric oxide in traumatic brain injury. Brain Pathol. 14, 195-201.

60. Anthony, D.C. and Couch, Y. (2014). The systemic response to CNS injury. Exp. Neurol. 258, 105-111.

61. Abrams, S.T., Zhang, N., Manson, J., Liu, T., Dart, C., Baluwa, F., Wang, S.S., Brohi, K., Kipar, A., Yu, W., Wang, G. and Toh, C.H. (2013). Circulating histones are mediators of trauma-associated lung injury. Am. J. Respir. Crit. Care Med. 187, 160-169.

62. Allam, R., Kumar, S.V., Darisipudi, M.N. and Anders, H.J. (2014). Extracellular histones in tissue injury and inflammation. J. Mol. Med. (Berl.) 92, 465-472.

TABLE 1. ACH-INDUCED DILATION IN MESENTERIC ARTERIES FROM CONTROL AND TBI RATS: PERCENT DILATION AND LOGEC50 VALUES

	Control			***TBI***		
Treatment	***Vasodilation elicited at ACh 1 µM (%)***	***LogEC$_{50}$***	**n**	***Vasodilation elicited at ACh 1 µM (%)***	***LogEC$_{50}$***	**n**
ACh	100 ± 1	−7.4 ± 0.01	5	59 ± 9*	−7.2 ± 0.4	7
+ L-NNA	46 ± 8*	−6.7 ± 0.5	5	55 ± 4	−6.6 ± 0.2	7
+ nor-NOHA	73 ± 9	−7 ± 0.3	5	98 ± 1*	−7 ± 0.06	6
+ L-arginine	79 ± 6*	−7.3 ± 0.3	5	95 ± 2*	−7 ± 0.4	6
+ L-sepiapterin	90 ± 7	−7.3 ± 0.3	5	91 ± 3	−6.8 ± 0.1	5

ACh, acetylcholine; EC, endothelial cell; L-NNA, Nω-nitro-L-arginine; nor-NOHA, Nω-hydroxy-nor-arginine.
ACh (1 µm), L-NNA (100 µm), nor-NOHA (20 µm), L-arginine (100 µm), L-sepiapterin (1 µm). Each value represents the mean ± SEM of *n* number of experiments. *$p < 0.0125$ versus the same group with Ach alone; Mann-Whitney test with Bonferroni correction.

FIGURES

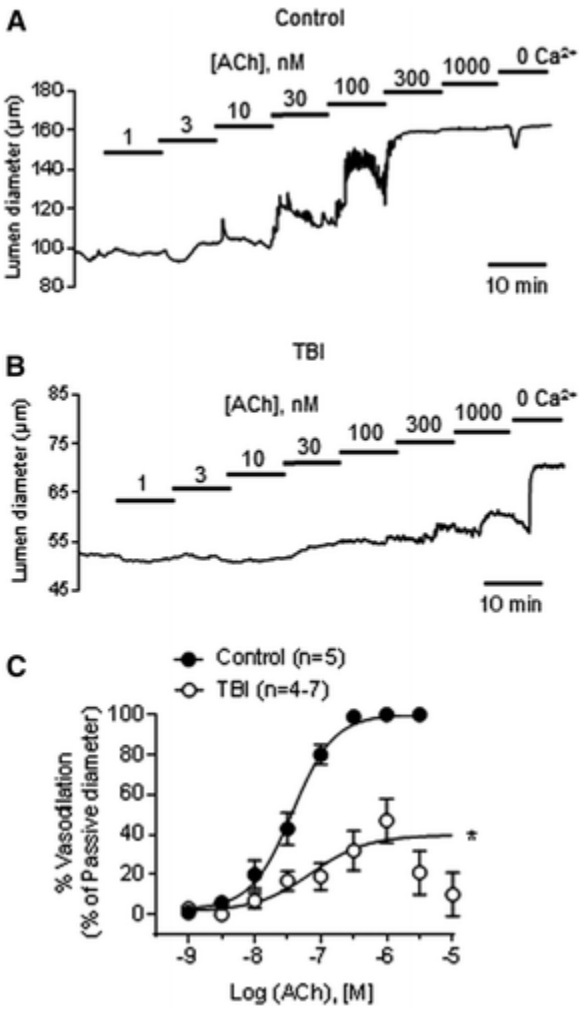

FIG. 1. Endothelial-dependent vasodilation is impaired after traumatic brain injury (TBI). Representative traces of acetylcholine (ACh) concentration-response curves in pressurized (80 mm Hg) mesenteric arteries from control ($n = 5$) and TBI ($n = 4–7$) rats in the absence (**A**) and presence (**B**) of the nitric oxide (NO) synthase inhibitor Nω-nitro-L-arginine (L-NNA) (100 µM). (**C**) Summary data for ACh concentration-response curves in arteries from control and TBI rats. *$p < 0.05$; two-way analysis of variance.

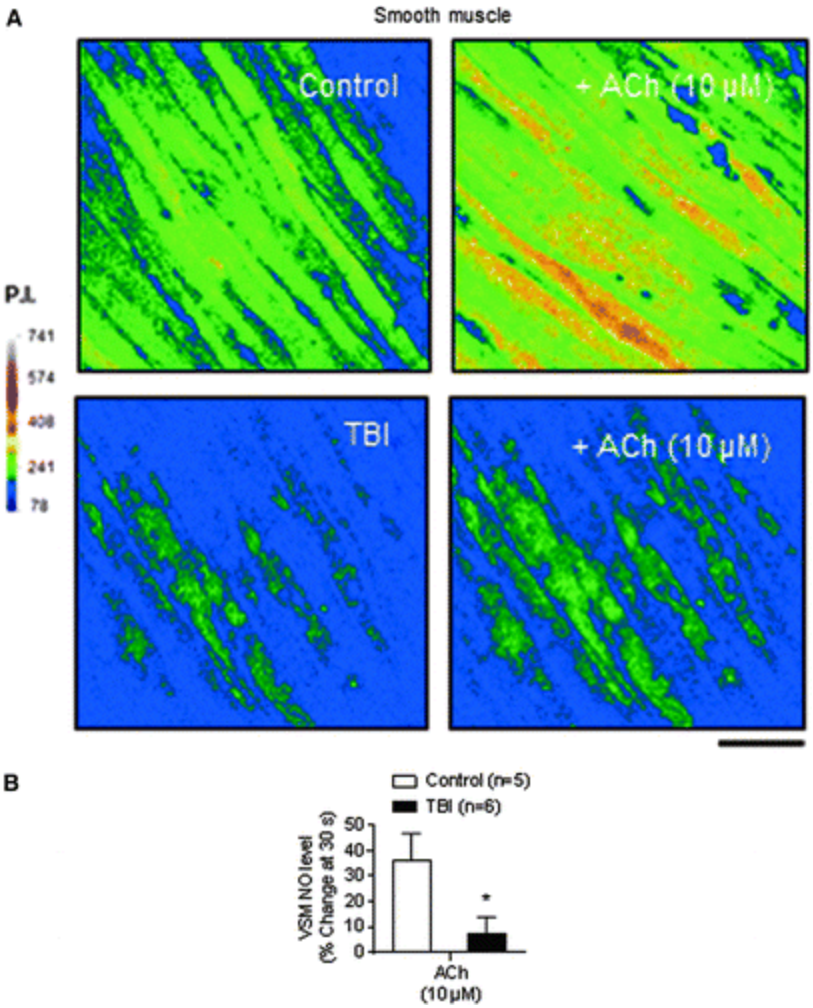

FIG. 2. Acetylcholine (ACh)-induced nitric oxide (NO) production is decreased after traumatic brain injury (TBI) in mesenteric arteries. (**A**) Basal and ACh-induced NO production in vascular smooth muscle (VSM) in mesenteric arteries (*en face* preparation) from control and TBI rats. Scale bar: 20 µm. (**B**) Summary data showing the percent change induced by ACh (10 µM) in VSM cells from control ($n = 4$) and TBI ($n = 4$) mesenteric arteries. *$p < 0.05$; Mann-Whitney test.

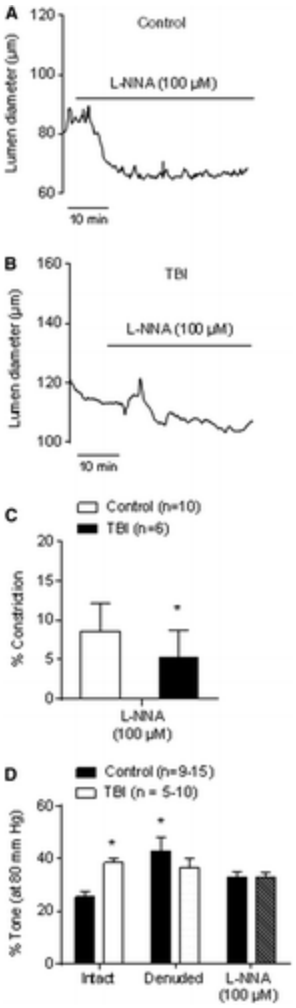

FIG. 3. Diminished endogenous nitric oxide (NO) production in mesenteric arteries from traumatic brain injury (TBI) animals causes enhanced myogenic tone. Representative traces of mesenteric arteries from control (**A**) and TBI (**B**) rats treated with the nitric oxide synthase (NOS) inhibitor Nω-nitro-L-arginine (L-NNA) (100 µM). The resulting vasoconstriction provides an additional index of endogenous NO production. (**C**) Summary data showing percent constriction of mesenteric arteries from control ($n = 10$) and TBI ($n = 6$) rats in response to L-NNA (100 µM). (**D**) Summary data showing percent tone elicited by 80 mm Hg in endothelium-intact and denuded arteries from control ($n = 9–15$) and TBI ($n = 5–10$) rats and intact arteries in the presence of L-NNA (100 µM). *$p < 0.05$ compared with control intact vessels; Mann-Whitney test.

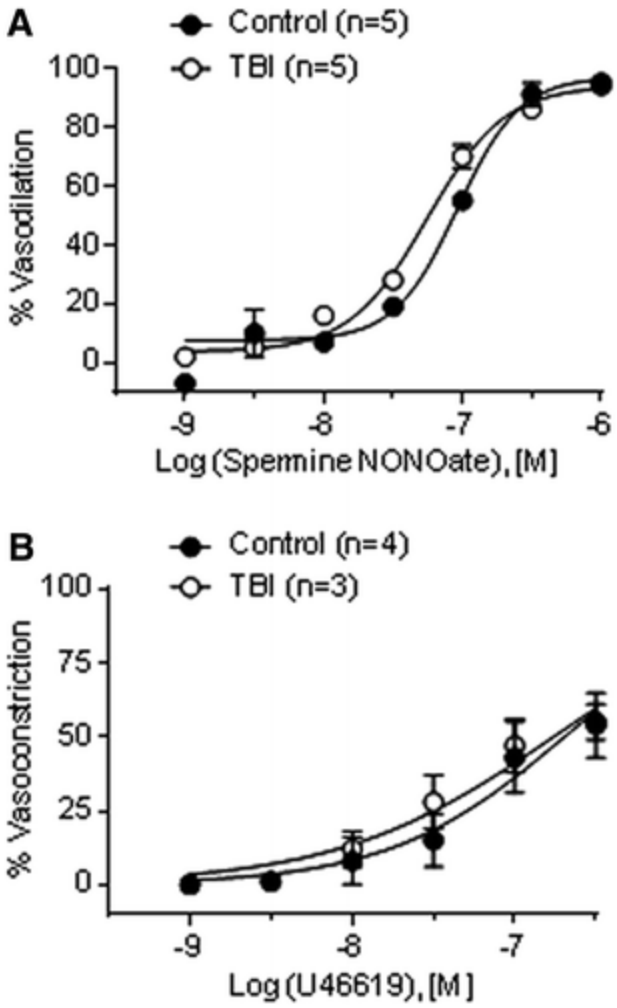

FIG. 4. Vascular smooth muscle sensitivity to nitric oxide (NO) and contractility are not altered after traumatic brain injury (TBI). (**A**) Sensitivity to NO was determined using the NO donor spermine NONOate (0.001–1 μM) in the presence of Nω-nitro-L-arginine (L-NNA) (100 μM) in pressurized (80 mm Hg) mesenteric arteries from control ($n = 5$) and TBI ($n = 5$) rats. (**B**) Smooth muscle contractility was determined by establishing U46619 concentration-response relationships in pressurized (40 mm Hg) mesenteric arteries from control ($n = 4$) and TBI ($n = 3$) rats.

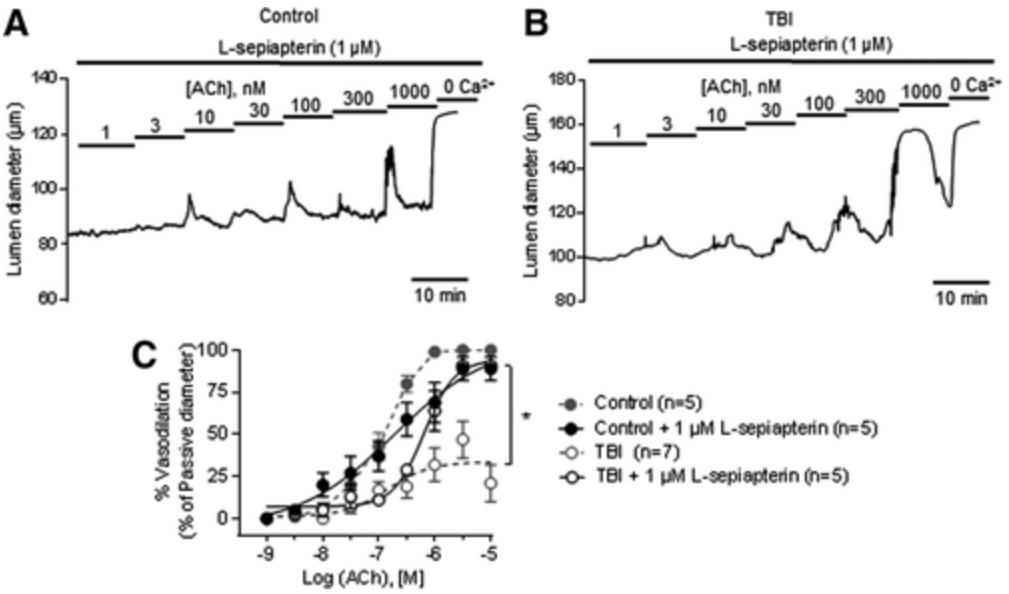

FIG. 5. Exogenous tetrahydrobiopterin (BH_4) supplementation improves acetylcholine (ACh)-induced dilation in traumatic brain injury (TBI) mesenteric arteries. Representative traces of ACh concentration-response curves in pressurized (80 mm Hg) mesenteric arteries from control (**A**) and TBI (B) rats in the presence of L-sepiapterin (1 μM). (**C**) Summary data showing ACh concentration-response curves in the presence of 1 μM L-sepiapterin from control and TBI ($n = 5$ each) rats. Dotted lines represent arteries from control and TBI rats previously shown in Figure 1. *$p < 0.05$; Two-way analysis of variance.

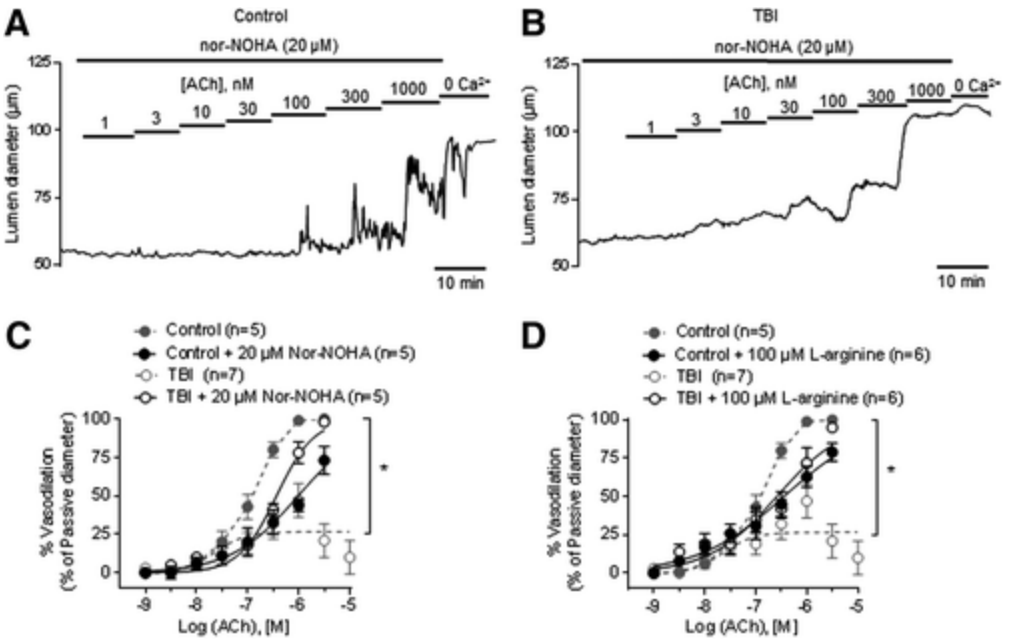

FIG. 6. Arginase inhibition and L-arginine supplementation improves acetylcholine (ACh)-induced dilation in traumatic brain injury (TBI) mesenteric arteries. Representative traces of ACh concentration-response curves in pressurized (80 mm Hg) mesenteric arteries from control (**A**) and TBI (**B**) rats in the presence of the specific arginase inhibitor Nω-hydroxy-nor-arginine (nor-NOHA) (20 µM). Summary data showing ACh concentration-response curves in the presence of 20 µM nor-NOHA (**C**) or 100 µM L-arginine (**D**) from control (n = 5–6) and TBI (n = 5–6) rats. Dotted lines represent arteries from control and TBI rats previously shown in Figure 1. *p < 0.05; Two-way analysis of variance.

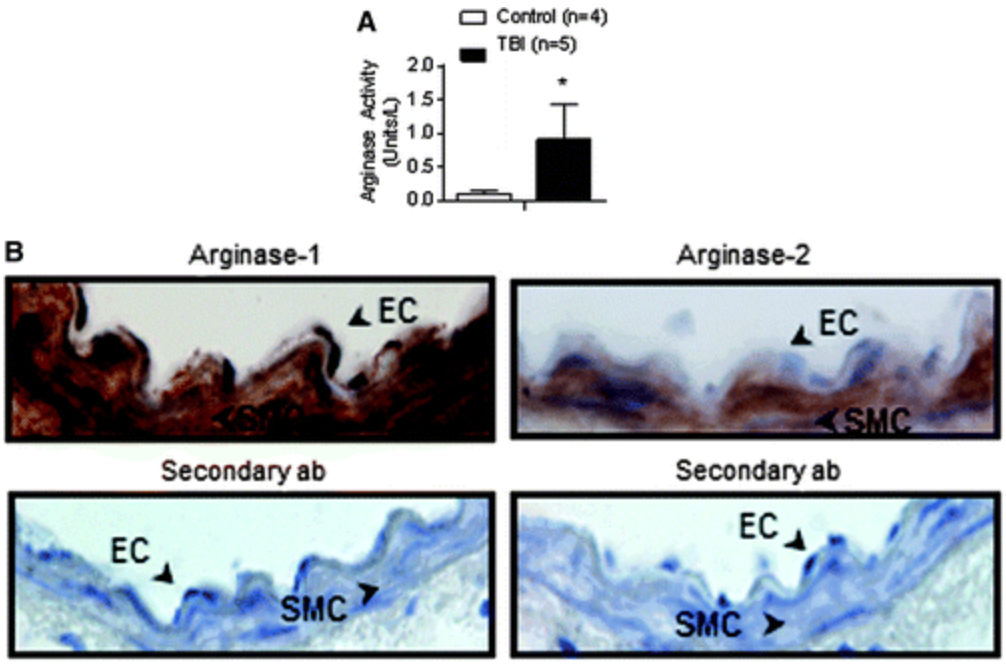

FIG. 7. Total arginase activity is increased after traumatic brain injury (TBI). (**A**) Arginase activity measured in homogenates of mesenteric arteries from control ($n = 4$) and TBI rats ($n = 5$) (**B**) Upper panels: Immunolocalization of Arg-1 and Arg-2 in mesenteric arteries from control animals. Arrows show staining in the vascular endothelium (EC) and smooth muscle cells (SMC). Lower panels: Control staining with secondary antibody alone. *$p < 0.05$; Mann-Whitney test.

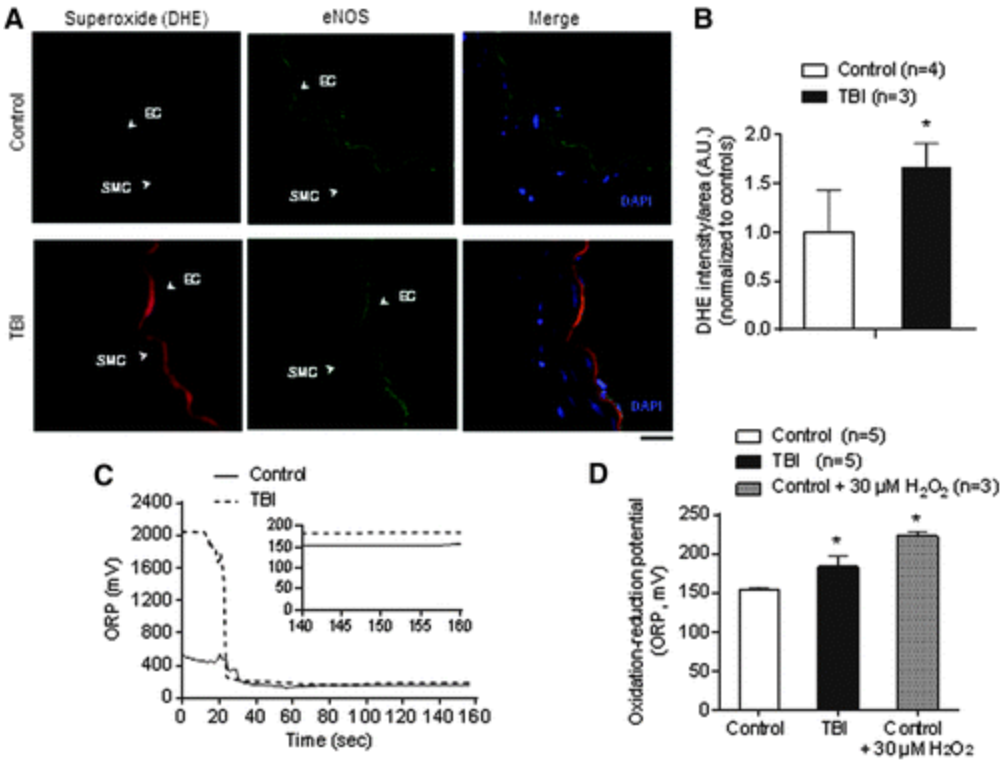

FIG. 8. Traumatic brain injury (TBI) rats show increased superoxide levels in the vascular endothelium and elevated oxidation-reduction potential (ORP) in plasma. (**A**) Representative images showing O_2^- levels measured by dihydroethidium (red, DHE stain) and endothelial nitric oxide synthase (eNOS) double-staining (green) in cross-sections obtained from mesenteric arteries from control and TBI rats. 4′-6-diamidino-2-phenylindole (DAPI) (blue) was used for nuclei staining. Scale bar: 20 µm. (**B**) Quantification of mean fluorescence intensity from control ($n = 4$) and TBI ($n = 3$) rats. Data within each group were normalized to controls (standardized to 1.0). (**C**) Representative ORP versus time traces. Plasma from a control rat (solid line) shows a potential measurement lower than a TBI (dotted line). The inset is a close-up of the final 20 sec reading. A static ORP measurement is the average value of the final 10 sec. (**D**) Summary data showing static ORP in plasma samples from control ($n = 5$) and TBI ($n = 6$) rats. Plasma from control rats treated with hydrogen peroxide (H_2O_2, 30 µM) was used as a positive control ($n = 3$). *$p < 0.05$; Mann-Whitney test. EC, vascular endothelium; SMC, smooth muscle cells.

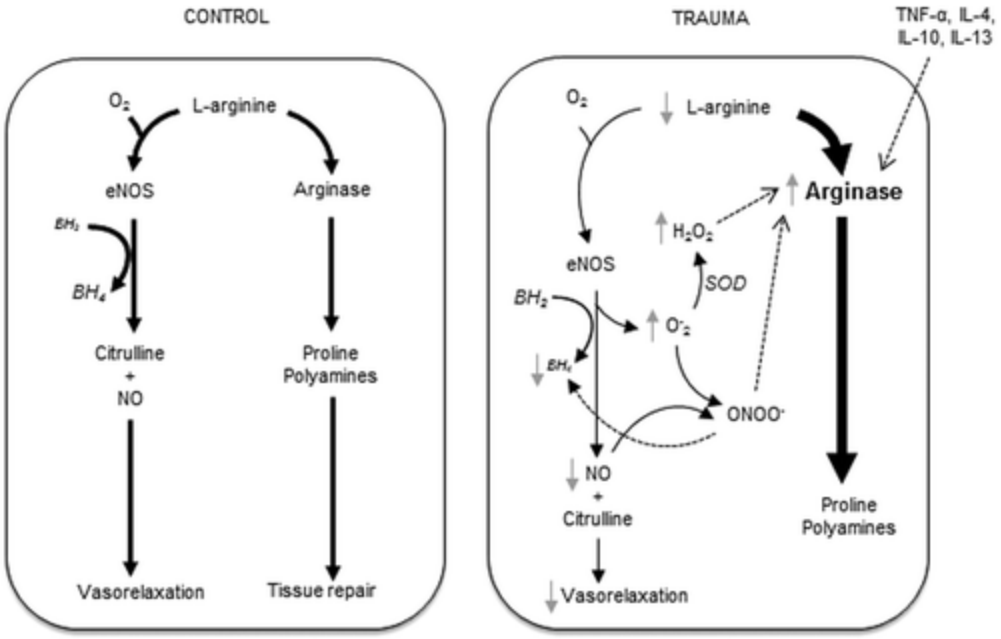

FIG. 9. Proposed mechanism for endothelial dysfunction after traumatic brain injury (TBI). Upregulated arginase-1 limits L-arginine availability to endothelial nitric oxide synthase (eNOS), leading to decreased nitric oxide (NO) production and O_2^- generation in the vascular endothelium. The excess O_2^- from uncoupled eNOS scavenges NO, forming peroxynitrites ($ONOO^-$) that rapidly oxidize tetrahydrobiopterin (BH_4) and propagate eNOS uncoupling. O_2^- is broken down by superoxide dismutases (SOD) into hydrogen peroxide (H_2O_2) and oxygen. The increase in production of H_2O_2 suppresses NO synthesis by increasing activity of arginase. The increased arginase activity consumes L-arginine and further uncouples eNOS promoting O_2^- production. These redox events with upregulation of endothelial arginase collectively contribute to the compromised vasodilation and increased myogenic tone observed after TBI.